Field cross correlator for analysis of ultrafast signals

K. Dou, A. Débarre, J.-L. Le Gouët, I. Lorgeré, and P. Tchénio

The cross-correlation function between two light fields is recorded with the help of a new device. The proposed correlator exhibits ultrashort time resolution. The optical path difference between the two interfering beams does not have to be known with interferometric precision. The experimental dynamic range proved to be as large as 10^5. The device features imaging capabilities that could be applied to the analysis of two-dimensional images with ultrashort time resolution.

Key words: Ultrashort time resolution, optical sampling, imaging interferometry.

1. Introduction

We provide a description and a demonstration of a field cross-correlation device that has been designed for the time-resolved analysis of ultrafast optical processes. Cross correlators are commonly used in optical sampling experiments in which one can sample the temporal shape of an ultrafast signal by scanning the delay between an optical probe pulse, which gives rise to signal emission, and an optical reference pulse, which triggers a detection gate.[1]

Optical gating can be achieved by mixing the signal with the delayed replica of the probe pulse in a nonlinear crystal and detecting the sum-frequency emission, which is known as intensity cross correlation.[2–4] The time resolution is given by the duration of the reference pulse.

Optically gated detection can also be accomplished by field cross correlation.[5–14] Then the signal amplitude is derived from the contrast of the fringes that result from interference with the reference field. Whereas the time resolution of intensity correlation is determined by the reference pulse duration, the relevant parameter in field correlation is the coherent time of light. This makes the latter technique attractive when broadband pulses are used, with coherence time much smaller than the pulse duration.

The authors are with the Laboratoire Aimé Cotton, Centre National de la Recherche Scientifique II, Bâtiment 505, 91405 Orsay Cedex, France. The permanent address for K. Dou is Changchun Institute of Physics, Chinese Academy of Sciences, 1 Yan'an Road, Changchun 130021, China.

Received 5 October 1993; revised manuscript received 9 May 1994.

0003-6935/94/347980-07$06.00/0.

Two standard ways have been used for the detection of an interference term. The first is well represented by the Michelson interferometer. Interference is revealed by the light intensity oscillation on the detector when the delay between the interfering beams is scanned.[5] The envelope of the oscillatory component coincides with the correlation function. Extraction of this function from the data requires the fulfillment of two conditions. At any recording time the length of the scan, with respect to the initial position of the device, has to be known with a precision that is much better than the precision of an optical wavelength. In addition, the same condition applies to the stability of the optical delay during the time needed to record one data point. The other classical approach to observe the interference term was first demonstrated by Thomas Young in 1801. This approach relies on detection of fringes that are built when the two beams of light are made to cross each other. The correlation function is related to the contrast of the spatial interference pattern. Less stringent conditions have to be met. Indeed the required precision on the optical path variation is given by $c\tau_c$, where τ_c is the coherence time of the light. This quantity is usually much larger than the optical wavelength. The strictness of the precision required of the delay is released at the expense of the resolution on the correlation function analysis. Whereas an optical period resolution is attained in a Michelson configuration, this parameter is multiplied by the number of recorded fringes in the case of the crossed-beam configuration.

The Young fringes can be recorded as a transient grating in a nonlinear material. The diffraction efficiency of a probe pulse on this grating is related to the fringe contrast and thus to the correlation func-

tion.[6–10] The interference pattern can also be detected directly on a photodiode array. The correlation function is then obtained by numerical calculation of the Fourier transform of the energy distribution on the detector.[11–13] Weak signals can be detected in this way without the spectral range limitation that applies to the nonlinear optical procedure. This detection of the weak signals is accomplished at the expense of time-consuming numerical processing. Both methods are incompatible with imaging interferometry[14] since each point of the source gives rise to a space-extended interference pattern.

Another approach should be mentioned, which does not require the observation of field-interference features but which preserves τ_c resolution. This approach is derived from the intensity interferometry, also known as two-photon interferometry, which has been extensively studied by Hanbury Brown and Twiss.[15] The limit on time resolution, which was determined by the detector response time, has been overcome recently.[16,17] However, because of the complex electronic photon-correlation procedure that should be needed to process each pixel, this technique does not seem to be appropriate for imaging interferometry.

We propose a correlator with imaging capabilities, which does not require any interferometric control of the optical path difference. In this device each point of the source gives rise to an interference signal that is received on a point photodetector, just as in a Michelson interferometer. But the interference term can be separated from the unmodulated background without varying the delay between the beams, just as in Young's configuration. Finally, signal processing is much faster than a Fourier transform.

In Section 2 we define autocorrelation and cross-correlation functions and describe the new correlator. In Section 3 we present and discuss an experimental test of the device.

2. Theoretical Description

A. Autocorrelation Function

The light pulse is represented by a classical electric field that reads

$$E(r, t) = E(t)\exp[i(\omega t - \mathbf{k}\cdot\mathbf{r})] + \text{c.c.}, \tag{1}$$

where $\mathbf{k}$ is a wave vector, and $E(t)$ is a slowly varying function of time, as compared with the optical period. The normalized autocorrelation function of the light field $E(t)$ is defined as

$$G(T) = \left|\int \mathrm{d}t E(t)E^*(t - T)\right| \Big/ \int \mathrm{d}t|E(t)|^2. \tag{2}$$

The correlation time is given by

$$\tau_C = \int \mathrm{d}t G(t). \tag{3}$$

We obtained the autocorrelation function by detecting the interference between the field and its delayed replica. For that purpose we split the initial field into two parts and adjusted the delay by varying the geometrical length of the optical paths before recombining the two fields on a detector. This interference term reads

$$\int \mathrm{d}t E(t)E^*(t - T)\exp[i\varphi(T)], \tag{4}$$

where $\varphi(T)$ stands for the relative phase shift between the two optical paths. According to the slowly varying envelope assumption the coherence time τ_c is much larger than the optical period $2\pi/\omega$. As a function of T, the interference term thus behaves as a slowly varying envelope $\int \mathrm{d}t E(t)E^*(t - T)$, which is modulated by the fast varying phase factor $\exp[i\varphi(T)]$. In a device such as the Michelson interferometer, in which delay T can be scanned with interferometric stability, the phase factor exhibits an oscillatory variation as a function of T and it can be removed easily by mere filtering.[5]

B. Field Cross Correlation

In the frame of the linear response theory, a sample that is illuminated by a probe field $E(t)$ radiates a signal $E_S(t)$ that is given by

$$E_S(t) = \int_0^\infty \mathrm{d}\tau E(t - \tau)L(\tau), \tag{5}$$

where $L(\tau)$ is the response function of the sample. To be specific, diffraction on a light-induced transient grating can be described in this way. Then the response function $L(\tau)$ can be expressed as the frequency-to-time Fourier transform of the grating diffraction efficiency.[12] In materials in which the width of the inhomogeneously broadened absorption band is much larger than the homogeneous linewidth, the response is not instantaneous. It spreads over an interval given by the lifetime of the optical dipoles. The signal is made to interfere with its parent field, $E_R(t) = E(t - T)$. The interference between these two fields is characterized by the cross-correlation function,

$$g(T) = \left|\int \mathrm{d}t E_S(t)E_R{}^*(t)\right| \Big/ \left[\int \mathrm{d}t|E_S(t)|^2 \int \mathrm{d}t|E_R(t)|^2\right]^{1/2}, \tag{6}$$

which can be expressed in terms of the response function $L(\tau)$ and the autocorrelation function $G(\tau)$ of the probe field $E(t)$:

$$g(T) = \left|\int_0^\infty \mathrm{d}\tau G(T - \tau)L(\tau)\right|. \tag{7}$$

When experimental conditions are such that the coherence time τ_c is much smaller than the characteristic time constant of $L(\tau)$, then $g(T)$ reduces to $L(T)$ and the field cross-correlation function gives direct access to the response function of the sample.[12,13] In the reverse situation, $g(T)$ coincides with the autocorrelation function $G(T)$.

C. Dual-Channel Field Cross Correlator

The principle of the dual-channel field cross correlator is illustrated in Fig. 1. The reference field R and the signal field S have linear orthogonal polarizations. The interference phenomenon is detected on photodiodes A and B, after splitting and mixing of the two fields on a half-transparent plate BS. P and $\lambda/4$ stand for an analyzer and a quarter-wave plate. Figure 1(b) shows the angular configuration of the signal and reference fields and of the analyzer and quarter-wave plate optical axes.

This setup is designed to achieve the simultaneous detection of two quadratures of the interference pattern of the signal and reference fields. It is derived from the so-called sigmameter,[18] a dual-channel Michelson interferometer that is used for the spectral calibration of monochromatic lasers.

On detector A, the transmitted part t_1R of the reference beam and the reflected part r_1S of the signal beam are combined together through a polarizer. The detected quantity, which is a function of delay T, is denoted A. It reads as follows:

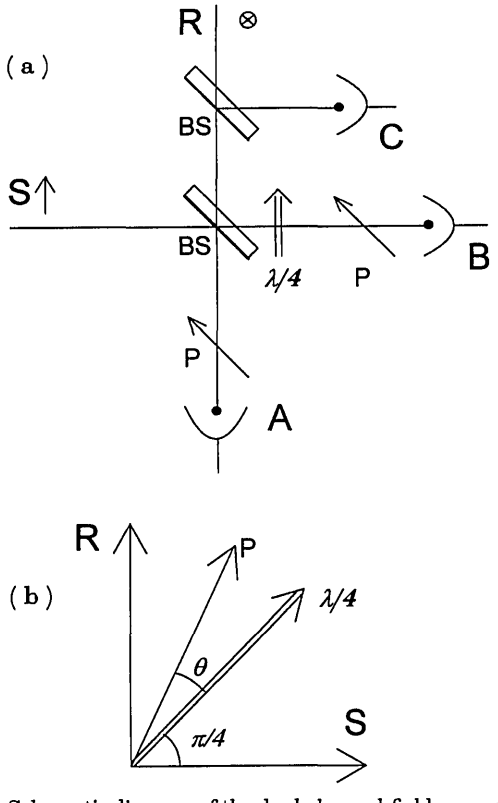

Fig. 1. Schematic diagram of the dual-channel-field cross correlator: S, R, signal and reference light fields with orthogonal polarization directions; BS, beam splitter; P, analyzer; $\lambda/4$, quarter-wave plate; A, B, UDT 455 photoelectric detectors.

$$A = \int dt' \, |t_1 R(t') + r_1 S(t')|^2. \tag{8}$$

If no phase shift were introduced by the beam splitter, a 90° dephasing between interference pattern detection A and B would be conveniently achieved by inserting a quarter-wave plate before detector B, with its optical axis aligned along the polarization of either the R or S field. A more refined configuration is needed to get rid of unavoidable phase shifts caused by the beam splitter.

Before reaching detector B, the transmitted part t_2S of the signal and the reflected part r_2R of the reference field go through a quarter-wave plate and then are recombined on a polarizer. The fixed optical axis of the $\lambda/4$ plate is set at 45° from the directions of both fields. The angle between the $\lambda/4$ plate and the polarizer is denoted θ. Then the detected quantity on B reads as follows:

$$\begin{aligned} B = \int dt' \, &|[r_2 R(t') - t_2 S(t')]\sin\theta \\ &+ i[r_2 R(t') + t_2 S(t')]\cos\theta|^2. \end{aligned} \tag{9}$$

Let φ_1 and φ_2 be the phase shifts produced by the beam splitter, which are defined in the following way:

$$\exp(i\varphi_1) = t_1 r_1^* / |t_1 r_1|, \tag{10}$$

$$\exp(i\varphi_2) = t_2 r_2^* / |t_2 r_2|. \tag{11}$$

Let ϕ denote the phase shift between the signal and the reference. The corresponding phase factor can be expressed as

$$\exp(i\phi) = \int dt R(t) S^*(t) \Big/ \left| \int dt R(t) S^*(t) \right|. \tag{12}$$

Thus Eqs. (8) and (9) can be rewritten as

$$\begin{aligned} A &= A_0 + A_1 + 2(A_0 A_1)^{1/2} g(T)\cos(\varphi_1 + \phi), \\ B &= B_0 + B_1 + 2(B_0 B_1)^{1/2} g(T)\sin(\varphi_1 + \phi), \end{aligned} \tag{13}$$

where

$$\begin{aligned} A_0 &= \int dt' |t_1|^2 |R(t')|^2, \\ A_1 &= \int dt' |r_1|^2 |S(t')|^2 \\ B_0 &= \int dt' |r_2|^2 |R(t')|^2, \\ B_1 &= \int dt' |t_2|^2 |S(t')|^2. \end{aligned} \tag{14}$$

The analyzer has been adjusted in such a way that θ satisfies the equation

$$\varphi_2 - 2\theta = \varphi_1 + \pi/2. \quad (15)$$

Combining Eqs. (13) one obtains the correlation function in the following form:

$$g(T) = [(A - A_0 - A_1)^2/4A_0A_1 + (B - B_0 - B_1)^2/4B_0B_1]^{1/2}, \quad (16)$$

which is expressed in terms of experimentally detected quantities and which does not depend on phase shift ϕ. The calibration parameters A_0, B_0, A_1, B_1 have to be measured in a preliminary stage by successively occulting the reference and signal beams. It is thus impossible to record these parameters and the cross-correlation-affected quantities A and B simultaneously. This degrades the calibration efficiency that is due to the light source intensity fluctuation. One can overcome this defect by permanently monitoring the intensity of a third detector, labeled C, and by the normalization of A and B by C. Then the normalized quantities $a = A/C$, $b = B/C$, $a_i = A_i/C$, $b_i = B_i/C$ $(i = 0, 1)$, which are unaffected by intensity fluctuation, are substituted into the expression of $g(T)$, which finally reads

$$g(T) = [(a - a_0 - a_1)^2/4a_0a_1 + (b - b_0 - b_1)^2/4b_0b_1]^{1/2}. \quad (17)$$

In the above calculation, the dispersive effect of the transparent media was not taken into account. Dispersion could affect the time resolution of the correlator. However, the two interfering beams essentially proceed along the same paths. The only imbalance is due to the glass plate that bears the beam-splitter coating. A compensating plate can be inserted to restore perfect balance between the different paths. Then the time resolution should be as small as an optical period, to be compared with that of correlators based on Young interference fringes.[6–13]

3. Results and Discussion

A. Experimental

We devote this subsection to the experimental evaluation of the cross correlator. In this simple test, the signal field does not result from the interaction of a probe pulse with a sample. Instead, an attenuated laser beam plays the role of the optical signal. This situation is described by Eq. (5), provided that the Dirac peak $\delta(\tau)$ is substituted for the response function $L(\tau)$. As depicted in Fig. 1, the field cross correlator includes two beam splitters, two Glan polarizers, a quarter-wave plate, and three photodiodes. The experimental setup is sketched in Fig. 2. We obtained the signal and reference fields by splitting a primary light beam that issues from a dye laser that is pumped by the second harmonic of a mode-locked YAG laser (Coherent Antares 76-YAG) at a repetition rate of 76 MHz. The dye laser pulse

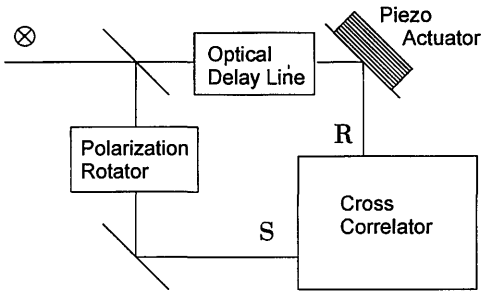

Fig. 2. Scheme of the test setup. The optical delay line on path R is adjusted with the help of a motorized translation stage.

duration amounts to a few picoseconds. The optical signals are detected on UDT 455 photodetectors, which incorporate a silicon photodiode chip and an operational amplifier. The response time of these detectors was adjusted to be approximately 5 μs. The electric signals were fed to three boxcar-gated integrators (Stanford Research System 250) that work in the single sample mode. The gate width is 15 μs. A translation stage was used to vary the delay between the reference and the signal pulses. It is driven by a stepping motor that varies the phase $\phi(T)$ in an uncontrolled way from step to step. Each step is 1 μm, which corresponds to a delay of 6.67 fs. A fine adjustment of the delay is provided by a piezoactuator, which can be used to vary continuously the optical path length on a submicrometer scale. The maximum rate of acquisition is limited by the computer processing time to approximately 200 Hz. However, most of the data have been recorded at a rate of 10 Hz, with six steps of the translation stage in the interval between two acquisitions.

B. Correlation Measurements

Two kinds of investigation have been undertaken. First, single-scan characteristics have been explored when the signal beam is approximately as intense as the reference beam, and results have been compared with those obtained with a single-channel correlator. Second, one has looked for the detectivity limit for multiple-scan recording.

The experimental procedure first requires us to determine the constant background contributions a_0, b_0, a_1, and b_1. These quantities, measured by cutting off the signal and the reference beams, are averaged over 100 acquisitions. Figure 3(a) displays the variation of the single-channel detected quantity $|a - a_0 - a_1|/2\sqrt{a_0a_1}$ when the piezoceramic continuously scans the optical delay T between the reference and the signal pulses over an interval of approximately 6.5 fs. Figure 4(a) displays the variation of the same single-channel function when the translation stage is scanned over 4000 steps, which corresponds to a delay of 26.7 ps. The noise that affects the profiles of the field autocorrelation function is due to the fluctuations of phase shift $\phi(T)$. They result from the mechanical instability of the setup. They also reflect the uncontrolled jump, which is accomplished by $\phi(T)$ at each step of the translation stage.

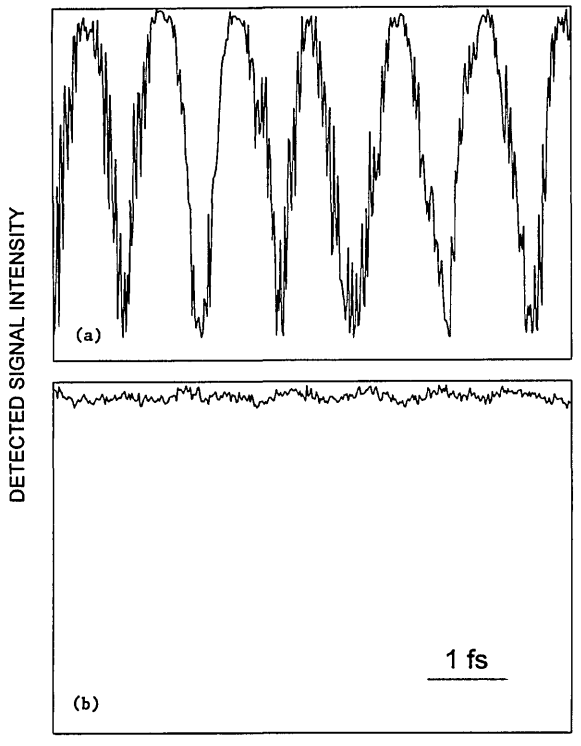

Fig. 3. Continuous scan of the optical delay by the piezoactuator. A path-difference variation of one wavelength leads to a 2π change in phase shift between the signal and the reference pulses. It can also be expressed as a delay variation of $\lambda/c = 2.07$ fs. (a) Oscillatory behavior of the correlation signal when a single detector is used. (b) Elimination of the fluctuations by dual-channel detection.

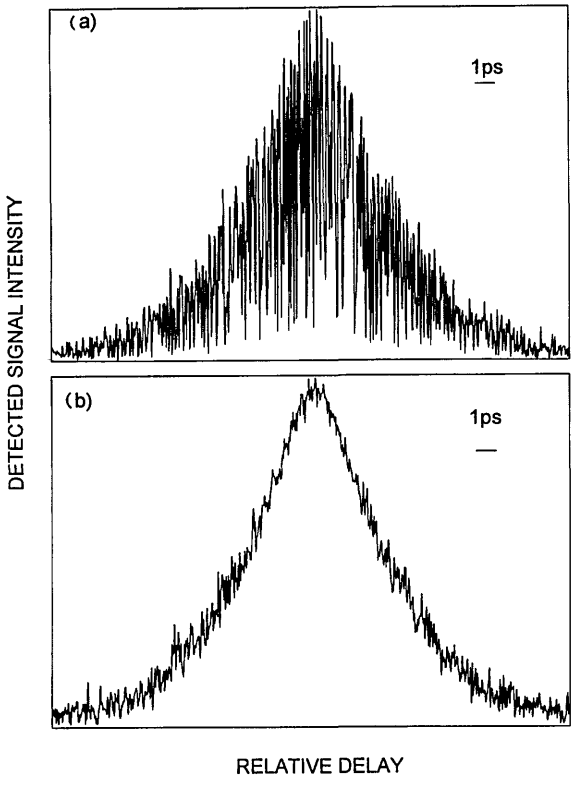

Fig. 4. Autocorrelation profiles obtained in a single scan of the translation stage without any average: (a) single-channel detection; (b) dual-channel detection.

The dual-channel detection is then installed. The orientation of the analyzer on channel B is adjusted. Voltage on the piezo is set so that minimum intensity is detected on photodiode A. The analyzer is rotated so that minimum intensity is simultaneously detected on photodiode B. A $\pi/2$ phase shift between the two channels is then achieved by an additional 45° rotation. Figure 3(b) displays the variation of the dual-channel signal,

$$[(a - a_0 - a_1)^2/4a_0a_1 + (b - b_0 - b_1)^2/4b_0b_1]^{1/2},$$

when the delay is varied over the same 6.5-fs interval as in Fig. 3(a). Figure 4(b) presents the variation of the same quantity when delay T is scanned over 26.7 ps, as in Fig. 4(a). These pictures demonstrate that the interference term is free of fluctuations caused by phase variations. All these recordings were obtained in a single scan of the delay line.

Averaging over six scans leads to the autocorrelation profile that is represented in Fig. 5(a). Satisfactory agreement is observed between experiment and the hyperbolic secant model of the laser field.[19,20] From this fit we deduced a coherence time of 6.7 ± 0.5 ps, which is consistent with the 7-ps value simultaneously measured by using the Fourier transform technique that we previously developed.[11]

A neutral density filter is inserted in the signal path in order to investigate the dynamic range of the device. Figure 5(b) shows experimental data obtained with various 10^{-D} attenuations. As D is increased the profiles get noisier with a larger background. However, for $D = 5.0$, we still successfully measured the correlation profile by averaging over 20 scans. The possible origin of the noise is considered and discussed in Subsection 3.C.

C. Discussion

Most intensity and phase fluctuations have been removed by the above-described procedure. However when the signal is weak, the interference term is more difficult to separate from noise. A model of this noise is proposed, which helps to elucidate its origins. We assume that the detected quantities a and b differ from their expectation value by some uncorrelated, zero-average, stochastic processes that are defined by

$$X = (a - \langle a \rangle)/a_0,$$
$$Y = (b - \langle b \rangle)/b_0, \tag{18}$$

where $\langle a \rangle$ and $\langle b \rangle$ stand for the expectation values of a and b. As a result, the recorded data, which is given by

$$I(T) = [(a - a_0 - a_1)^2/4a_0a_1 + (b - b_0 - b_1)^2/4b_0b_1]^{1/2}, \tag{19}$$

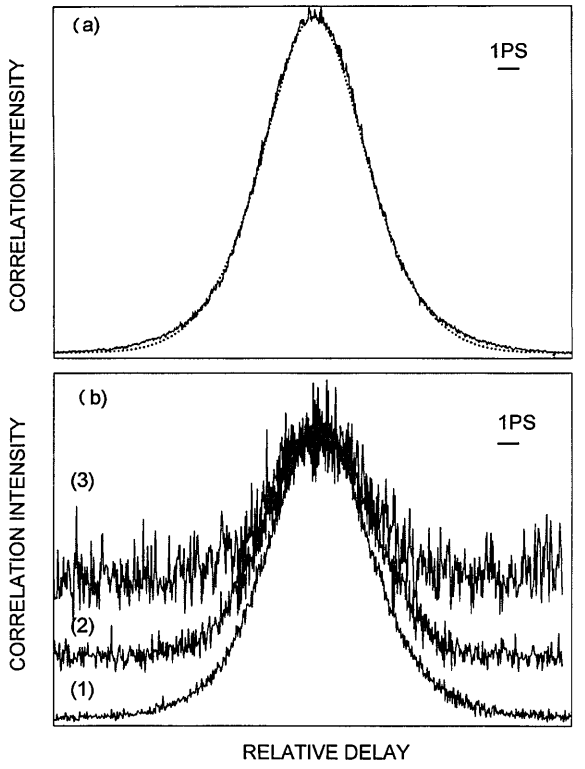

Fig. 5. Averaged correlation profiles for different values of the optical density inserted on the signal path: (a) experimental (solid) and theoretical (dashed) curves for $D = 0$ plotted together. The average was taken over six scans. (b) Signals of the field cross correlation averaged over approximately 20 times for (1) $D = 2$, (2) $D = 4$, and (3) $D = 5$.

can be expressed in the following form:

$$I(T) = \{g(T)^2 + g(T)[X\sqrt{a_0/a_1}\cos(\Psi) + Y\sqrt{b_0/b_1}\sin(\Psi)] + (X^2a_0/a_1 + Y^2b_0/b_1)/4\}^{1/2}, \quad (20)$$

where $\Psi = \varphi_1 + \phi$. In the absence of fluctuation ($X = Y = 0$), $I(T)$ exactly equals $g(T)$. For the sake of simplicity we consider the statistical variable $S = I(T)^2$ instead of $I(T)$. The standard deviation for S is defined as

$$\sigma_S^2 = \langle S^2\rangle - \langle S\rangle^2. \quad (21)$$

The stochastic processes X and Y are assumed to be Gaussian. The standard quadratic deviations are denoted as

$$\langle X^2\rangle = \sigma_X^2, \qquad \langle Y^2\rangle = \sigma_Y^2. \quad (22)$$

Then the first two statistical moments of S read as follows:

$$\langle S\rangle = g^2 + (1/4)(\sigma_X^2 a_0/a_1 + \sigma_Y^2 b_0/b_1), \quad (23)$$

$$\langle S^2\rangle = g^4 + g^2\{\sigma_X^2[\cos^2(\Psi) + 1/2]a_0/a_1 + \sigma_Y^2[\sin^2(\Psi) + 1/2]b_0/b_1\} + (3/16)[\sigma_X^4(a_0/a_1)^2 + \sigma_Y^4(b_0/b_1)^2] + (1/8)\sigma_X^2\sigma_Y^2 a_0b_0/(a_1b_1). \quad (24)$$

The standard deviation can be expressed in terms of $\langle S\rangle$ in the following way:

$$\sigma_S^2 = k_1\langle S\rangle - k_0, \quad (25)$$

where

$$k_1 = \sigma_X^2\cos^2(\Psi)a_0/a_1 + \sigma_Y^2\sin^2(\Psi)b_0/b_1, \quad (26)$$

$$k_0 = (1/4)[\sigma_X^2\cos^2(\Psi)a_0/a_1 + \sigma_Y^2\sin^2(\Psi)b_0/b_1] \times (\sigma_X^2 a_0/a_1 + \sigma_Y^2 b_0/b_1) - (1/8)[\sigma_X^4(a_0/a_1)^2 + \sigma_Y^4(b_0/b_1)^2]. \quad (27)$$

When the time delay is scanned, the Ψ phase angle fluctuates. Thus $\cos^2\Psi$ and $\sin^2\Psi$ can be replaced by their average value of 1/2 in Eqs. (26) and (27), so that k_0 and k_1 are reduced to

$$k_1 = (1/2)(\sigma_X^2 a_0/a_1 + \sigma_Y^2 b_0/b_1), \quad (28)$$

$$k_0 = (1/4)(\sigma_X^2\sigma_Y^2 a_0b_0/a_1b_1). \quad (29)$$

The standard deviation σ_S^2 appears to be a linear function of $\langle S\rangle$. Experimental data are in good agreement with this prediction as shown in Fig. 6 for $D = 5.0$. Best fit is obtained for $k_1 = 0.30$ and $k_0 = 0.005$.

The expression for $\langle S\rangle$ [Eq. (23)] indicates that, in the far wings of the correlation function, when $g \to 0$, the quantity $\langle S\rangle$ tends to a residual background $\langle S_0\rangle$, which reads as follows:

$$\langle S_0\rangle = (1/4)(\sigma_X^2 a_0/a_1 + \sigma_Y^2 b_0/b_1). \quad (30)$$

The slope k_1 is related to the background $\langle S_0\rangle$ by

$$k_1/\langle S_0\rangle = 2. \quad (31)$$

This property can be checked on the experimental profiles. For $D = 5$, the background measured in Fig. 7 is $\langle S_0\rangle = 0.15$, whereas, according to Fig. 6, $k_1 =$

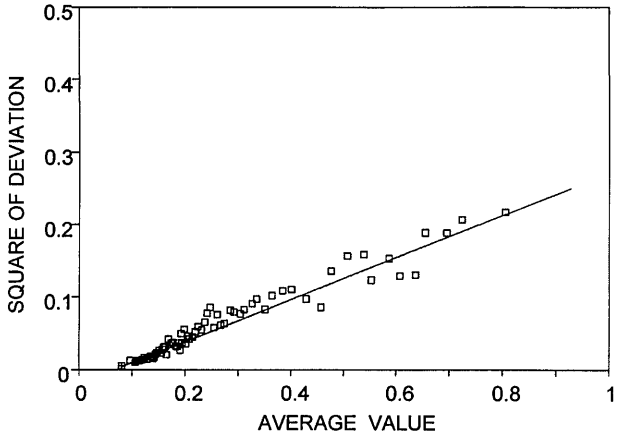

Fig. 6 Dependence of the square deviation σ_S^2 on the average intensity $\langle S\rangle$ is linear and the slope was obtained as $k_1 = 0.29$.

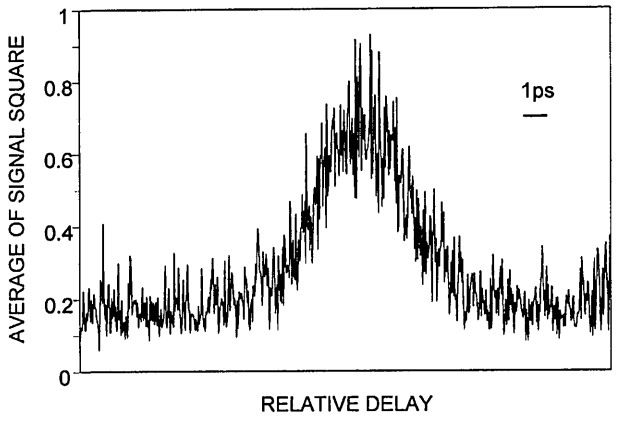

Fig. 7. Background of the average intensity $\langle S \rangle$ versus the relative time delay measured as $\langle S_0 \rangle = 0.15$ for $D = 5$.

0.29. Thus $k_1/\langle S_0 \rangle = 1.93$, which is close to the expected value of this ratio. When $D = 5$, the ratios a_0/a_1 and b_0/b_1 are, respectively, measured to be $a_0/a_1 = 1.26 \times 10^5$ and $b_0/b_1 = 6.94 \times 10^5$, and with Eqs. (24) and (25) we obtain $\sigma_X = 1.2 \times 10^{-3}$ and $\sigma_Y = 8 \times 10^{-4}$. It should be noted that parameters a and b include normalization of A and B signals by the laser intensity detected on C. We have checked to determine that the fluctuations of a and b are not correlated with the laser intensity fluctuations. When the channels A and C gated integrators are fed with the single signal that issues from photodiode A, the residual standard deviation on A/C is measured to be 7×10^{-4}. The same result applies to parameter b. These quantities correspond to the noise that is due only to the boxcar integrators. Values obtained for σ_X and σ_Y with $D = 5$ are close to this electronic limit, which appears to be the main source of noise.

4. Conclusion

A new method for measuring the field cross correlation has been demonstrated theoretically and experimentally. The response time of the detectors and of the electronics does not limit the time resolution of the proposed device. Picosecond pulses have been used to check it. However the correlator should work, without any change, in the femtosecond range. Despite the interference nature of the recorded signal, the optical path difference between the correlated beams does not have to be controlled with interferometric precision. Processing the data does not require lengthy computing, and it takes only a few seconds to record the correlation profile of 640 points. Finally, the two point detectors that were used in this demonstration could be substituted with photodetector matrices, opening the way for an analysis of two-dimensional images with ultrashort time resolution.

References

1. E. P. Ippen and C. V. Shank, "Techniques for measurement," in *Ultrashort Light Pulses: Picosecond Techniques and Applications,* S. L. Shapiro, ed. (Springer-Verlag, Berlin, 1977), pp. 83–122.
2. M. A. Duguay and J. W. Hansen, "Optical sampling of subnanosecond light pulses," Appl. Phys. Lett. **13,** 178–180 (1968).
3. J. E. Rothenberg, D. Grischkowsky, and A. C. Balant, "Observation of the formation of the 0π pulse," Phys. Rev. Lett. **53,** 552–555 (1984).
4. A. Rebane, J. Aaviskoo, and J. Kuhl, "Storage and time reversal of femtosecond light signals via persistent spectral hole burning holography," Appl. Phys. Lett. **54,** 93–95 (1989).
5. C. Joubert, M.-L. Roblin, and R. Grousson, "Temporal reversal of picosecond optical pulses by holographic phase conjugation," Appl. Opt. **28,** 4604–4612 (1989).
6. H. J. Eichler, U. Klein, and D. Langhans, "Coherence time measurement of picosecond pulses by light-induced grating method," Appl. Phys. Lett. **21,** 215–219 (1980).
7. R. Trebino, E. K. Gustafson, and A. E. Siegman, "Fourth-order partial-coherence effects in the formation of integrated intensity gratings with pulsed light sources," J. Opt. Soc. Am. B **3,** 1295–1304 (1986).
8. W. L. Nighan, T. Gong, L. Liou, and P. M. Fauchet, "Self-diffraction: a new method for characterization of ultrashort laser pulses," Opt. Commun. **69,** 339–344 (1989).
9. A. S. L. Gomes, L. H. Acioli, C. de Araujo, and J. Rios Leite, "Dispersion of coherence spikes of incoherent broadband dye lasers," Opt. Commun. **73,** 475–478 (1989).
10. V. Dominic, X. S. Yao, R. M. Pierre, and J. Feinberg, "Measuring the coherence length of mode-locked laser pulses in real time," Appl. Phys. **56,** 521–523 (1990).
11. A. Débarre, J. C. Keller, J. L. Le Gouët, A. Richard, and P. Tchénio, "An amplitude correlator for broadband laser source characterization," Opt. Commun. **73,** 309–313 (1989).
12. A. Débarre, J. C. Keller, J. L. Le Gouët, and P. Tchénio, "Field cross-correlation retrieval of optically stored data," J. Opt. Soc. Am. B **8,** 153–159 (1991).
13. M. A. Bouchene, A. Débarre, J. C. Keller, J. L. Le Gouët, and P. Tchénio, "Observation of 0π-pulse formation with incoherent light," J. Opt. Soc. Am. B **9,** 281–289 (1992).
14. J.-P. Maillard and D. Simons, "First results of an imaging FTS with a NICMOS camera," in *Proceedings of the ESA Workshop on Solar Physics and Astrophysics at Interferometric Resolution,* L. Damé and T. D. Guyenne, eds. (European Space Agency, Noordwijk, The Netherlands, 1992), ESA SP-344, pp. 205–210.
15. R. Hanbury Brown and R. Q. Twiss, "Correlation between photons in two coherent beams of light," Nature (London) **177,** 27–29 (1956).
16. Z. Y. Ou, E. C. Gage, B. E. Magill, and L. Mandel, "Fourth-order interference technique for determining the coherence time of a light beam," J. Opt. Soc. Am. B **6,** 100–103 (1989).
17. Y. Miyamoto, T. Kuga, M. Baba, and M. Matsuoka, "Measurement of ultrafast optical pulses with two-photon interference," Opt. Lett. **18,** 900–902 (1993).
18. P. Juncar and J. Pinard, "Instrument to measure wave numbers of cw and pulsed laser lines: the sigmameter," Rev. Sci. Instrum. **53,** 939–948 (1982).
19. H. A. Haus, "Theory of mode locking with a slow saturable absorber," IEEE J. Quantum Electron. **QE-11,** 736–746 (1975).
20. H. A. Haus, C. V. Shank, and E. P. Ippen, "Shape of passively mode-locked laser pulses," Opt. Commun. **15,** 29–31 (1975).